Influence of strain rate on the mechanical behavior of cortical bone interstitial lamellae at the micrometer scale

Maximilien Vanleene
Laboratoire de Biomécanique et Génie Biomédical, CNRS UMR 6600 (Centre National de la Recherche Scientifique Unité Mixte de Recherche), Université de Technologie de Compiègne, 60205 Compiègne Cedex, France

Pierre-Emmanuel Mazeran
Laboratoire Roberval Unité de Recherche en Mécanique, CNRS FRE 2833 (Centre National de la Recherche Scientifique Formation de Recherche en Evolution 2833), Université de Technologie de Compiègne, 60205 Compiègne Cedex, France

Marie-Christine Ho Ba Tho[a)]
Laboratoire de Biomécanique et Génie Biomédical, CNRS UMR 6600 (Centre National de la Recherche Scientifique Unité Mixte de Recherche), Université de Technologie de Compiègne, 60205 Compiègne Cedex, France

(Received 21 December 2005; accepted 3 May 2005)

Investigations of bone mechanical properties are of major importance for bone pathology research, biomaterials, and development of in vivo bone characterization devices. Because of its complex multiscale structure, assessment of bone microstructure is an important step for understanding its mechanical behavior. In this study, we have investigated the strain rate influence on the mechanical properties of interstitial lamellae on two human femur bone samples. Nanoindentation tests were performed with the continuous stiffness measurement technique. Young's modulus and hardness were calculated using the Oliver and Pharr method. A statistical significant influence of strain rate on hardness was found ($p < 0.05$) showing a viscoplastic behavior of interstitial bone at the micrometer scale. This phenomenon may reflect the role of the organic component in the bone matrix mechanical behavior.

I. INTRODUCTION

Mechanical properties of bone are of importance in understanding bone pathologies, to develop biomimetic materials and in vivo bone characterization devices. Cortical bone is described as a very complex material with a multiscale hierarchical architecture: molecular level (matrix of collagen fibrils and apatite crystals), tissue level (haversian system), and organ level (trabecular and cortical bones).[1]

Bone mechanical behavior resulting from this complex structure has been widely investigated at the macroscale level over the last forty years, using classical mechanical tests (tensile, compressive, torsion and bending)[2–6] or ultrasonic tests (transmission, reflection).[7–9] Heterogeneity, anisotropy, and elastoviscoplastic behavior of bone tissue have been demonstrated. However, few investigations have been performed at the microstructural level.[10–13]

The recent development of the nanoindentation technique[14–16] has allowed the investigation of bone mechanical behavior at the lamella level. At this micrometer scale, a difference of mechanical properties between cortical and trabecular bones has been observed.[17–19] Moreover, differences of mechanical properties have been observed between osteon and interstitial lamellae and also within osteon lamellae.[20–23] The investigation of bone anisotropy at the lamella scale has also been conducted on human and bovine specimens.[24,25] The study of bone viscoelasticity of the osteon lamellae has been conducted only once by Fan et al. on a human dry specimen.[26] Finally, an investigation was performed recently by Tai et al.[27] on the plastic residual deformation of collagen fibrils after nanoindentation tests on bovine bone. Demineralization effects on this plastic behavior were also investigated.

During investigations of bone samples, the bone specimen preparation (wet, dry, dehydrated, embedded or not, demineralized) and nanoindentation operating conditions (indentation depth, loading rate, repetitive loading, time delay)[16,28,29] must be considered for the assessment of mechanical properties.

The aim of the present study was to investigate the time dependent mechanical behavior of the interstitial lamellae of human cortical bone using a dynamic nanoindentation technique at different strain rates.

II. MATERIALS AND METHODS

Bone cortical specimens were obtained from a male human femur (70 years old). Samples were cut

[a)]Address all correspondence to this author.
e-mail: hobatho@utc.fr
DOI: 10.1557/JMR.2006.0255

($5 \times 5 \times 4$ mm) from the medial and lateral parts of a transversal femur section using a diamond saw in the wet condition. Specimens were dried in air at room temperature. Upper transversal faces of samples were ground using abrasive papers of decreasing grit sizes (P800, P1200) and polished on microcloths with alumina suspensions (1, 0.3, and 0.02 μm particle sizes). Samples were then cleaned with an ultrasound cleaner ten minutes in distilled water and dried at room conditions (temperature: 18–22 °C, humidity = 40 ± 5%).

Nanoindentation tests were performed with a Nano indenter XP (MTS System Corp., Oak Ridge, TN) using a Berkovich indenter. The Nano indenter XP system has a load and displacement resolution of 50 nN and 0.01 nm, respectively. Indentations were performed at constant quasistatic strain rate in the longitudinal direction of the femur diaphysis using the continuous stiffness measurement (CSM) method.[14] This method consists of superimposing a high-frequency small oscillation on the quasistatic component of the loading. The depth oscillation was controlled at 2 nm with a 45 Hz frequency. The ratio of the oscillation load to the oscillation displacement gave the harmonic contact stiffness. The Young's modulus and hardness were calculated using the Oliver and Pharr method.[14] Using the Nanoindenter XP, we were able to test the influence of a variation of the strain rate applied during the nanoindentation on the mechanical properties.[15] As hardness was related to the plastic deformation of the tested material, the evolution of hardness with the strain rate applied could be attributed to a viscoplastic behavior of the bone material.

The calibration of the nanoindenter geometry was done with a fused silica sample (E = 72 GPa, H = 10 GPa) allowing an accurate measurement of the Young's modulus and hardness for homogeneous materials and for indentation depth superior to 20 nm (Fig. 1).

Ten and six interstitial lamellae locations were chosen on the lateral and the medial specimens, respectively. For each location, nine indentation tests were conducted consisting of sets of three indentations (separated by 50 μm) at three different strain rates ($\dot{\epsilon}$): 0.005, 0.05, and 0.5 s^{-1} (Fig. 2). Indentation tests were depth controlled from 0 to 3000 nm. The bone Poisson's ratio was fixed at 0.3. This value has been commonly used in nanoindentation studies.[17,19] A variation of 0.1 around this 0.3 value has an impact of 7.7% on the computed value of Young's modulus. A total of 144 indents were performed.

Statistical analyses were performed to investigate the difference of Young's modulus and hardness between samples for the different strain rates. Moreover, regression analyses allowed investigation of the relationships between Young's modulus and hardness as a function of the indentation strain rates. Statistical tests were performed using the software Statgraphics plus version 5.0 (Statistical Graphics Corp, Herndon, VA).

III. RESULTS

Typical Young's modulus assessment of fused silica as a function of tip displacement into surface exhibited an artifact of measurement from 0 to about 20 nm followed by a stable value until the end of the nanoindentation test (Fig. 1).

Measurements on bone exhibited the same phenomenon as illustrated in Fig. 3. The mechanical properties could not be calculated accurately for low indentation depth (<200 nm). The measured mechanical properties were not constant until a depth indentation varying from 200 to 1500 nm reflecting the heterogeneity of bone. To avoid this phenomenon, our measurements were collected from the average values in the range of 2000–3000 nm indentation depths for any strain rate.

Statistically significant differences between the lateral and the medial specimens were observed for hardness values at all strain rates ($p < 0.05$). For Young's modulus, a significant difference was found only for

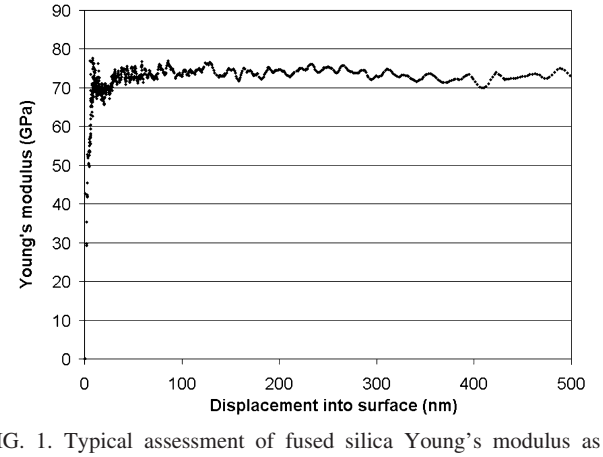

FIG. 1. Typical assessment of fused silica Young's modulus as a function of the displacement into the surface at strain rate $\dot{\epsilon}$ = 0.05 s^{-1}.

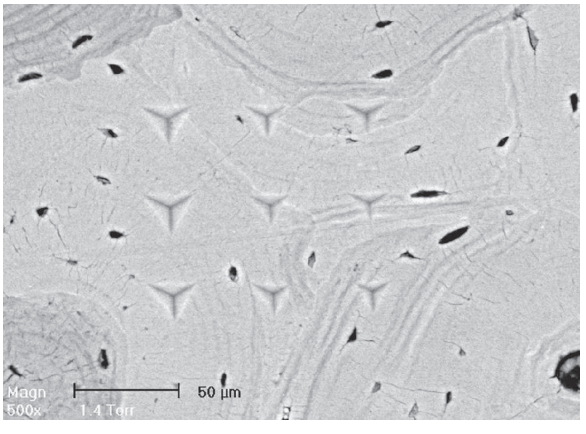

FIG. 2. ESEM image of the nanoindentation matrix in the interstitial lamellae. From left to right, indentations at strain rate $\dot{\epsilon}$ = 0.5, 0.05, and 0.005 s^{-1}.

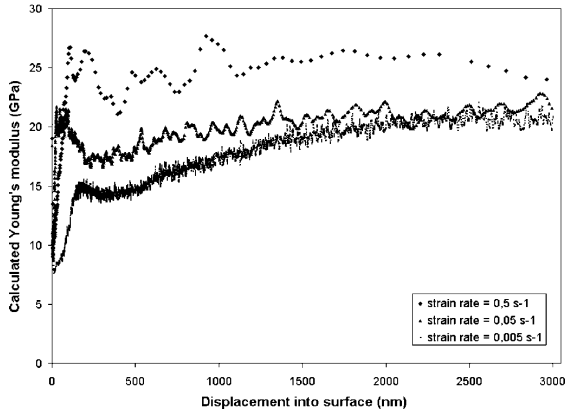

FIG. 3. Typical measurement of Young's modulus in bone sample as a function of the displacement into surface at strain rate $\dot{\epsilon} = 0.5\ s^{-1}$, $\dot{\epsilon} = 0.05\ s^{-1}$, and $\dot{\epsilon} = 0.005\ s^{-1}$.

$\dot{\epsilon} = 0.05\ s^{-1}$ ($p < 0.05$). Mean, standard deviation, and minimum and maximum values of Young's modulus and hardness assessed from 2000 to 3000 nm in the two bone samples for the different strain rates are summarized in Table I.

An increase of mechanical properties was observed with increasing strain rates. In fact, for each bone specimen, Analysis of Variance (ANOVA) tests showed a significant difference between mechanical properties measured at the different strain rates.

Relationships between calculated Young's modulus and hardness as a function of strain rate are given below:

for the lateral specimen:

$$E = 25.74 \times \dot{\epsilon}^{0.026} \qquad R^2 = 0.9 \quad , \tag{1}$$

$$H = 1.1 \times \dot{\epsilon}^{0.081} \qquad R^2 = 0.98 \quad ; \tag{2}$$

for the medial specimen:

$$E = 24.83 \times \dot{\epsilon}^{0.032} \qquad R^2 = 0.98 \quad , \tag{3}$$

$$H = 0.95 \times \dot{\epsilon}^{0.099} \qquad R^2 = 0.97 \quad . \tag{4}$$

TABLE I. Mechanical properties assessed at different strain rates in the lateral and medial specimens (mean ± standard deviation, minimum–maximum)

Bone specimen strain rate (s^{-1})	Calculated Young's modulus (GPa)		Calculated hardness (GPa)	
	Lateral	Medial	Lateral	Medial
0.005	22.15 ± 2.1	21.11 ± 1.97	0.7 ± 0.13[a]	0.55 ± 0.09[a]
	17.26–26.44	17.06–24.42	0.53–0.98	0.36–0.71
0.05	24.34 ± 1.58[a]	22.33 ± 2.22[a]	0.88 ± 0.07[a]	0.74 ± 0.12[a]
	21.71–27.85	18.62–24.8	0.77–1.03	0.61–0.98
0.5	25 ± 3.07	24.43 ± 1.93	1.02 ± 0.13[a]	0.87 ± 0.14[a]
	18.95–30.8	21.11–28.52	0.76–1.31	0.63–1.07

[a]Statistical significant difference $p < 0.05$.

These relationships are illustrated in Figs. 4 and 5.

IV. DISCUSSION

As observed on the reference sample of fused silica for the first 20 nm of indentation, an accurate measurement of the Young's modulus and hardness could not be achieved at low indentation depth (<20 nm). This phenomenon was attributed to the imperfect geometry of the indenter known as the tip defect.[30] This defect had an impact on the estimation of the contact depth during the first nanometres of the tip penetration into the surface. It was minimized as the depth increased. This implied an error on the contact area estimation and thus on the reduced modulus of the material. In comparison with fused silica, the artifact depth range was more important in bone samples and was attributed to the surface roughness, surface treatments, and surface forces. This was related to the great difficulties of preparing accurate surfaces for biologic specimens without inducing modifications of the material.

Young's modulus and hardness values measured in the region from 200 to 1500 nm were not found to be constant. It may be related to the bone heterogeneity at the micrometer scale and to the surface material alteration by the sample preparation (cutting, polishing), drying, and surface oxidation. Constant values were observed above 1500 nm. Average values of Young's modulus and hardness from 2000 to 3000 nm were calculated to observe the global response of bone interstitial lamellae when the indentation strain rate was modified.

The values of Young's modulus and hardness of bone interstitial lamellae observed from 2000 to 3000 nm were within the same range as those found in the literature.[19,20] The statistically significant difference ($p < 0.05$) found between values of hardness from the medial and lateral specimens seems to illustrate the heterogeneity of bone between different locations in the same bone.

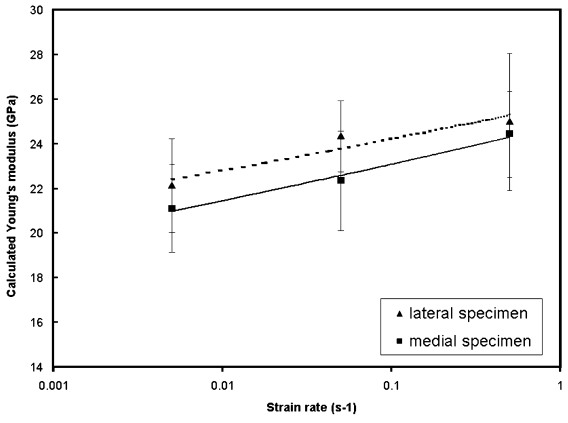

FIG. 4. Variation of calculated Young's modulus as a function of strain rate in bone specimens (average values from 2000 to 3000 nm indentation depth; error bars correspond to the standard deviation).

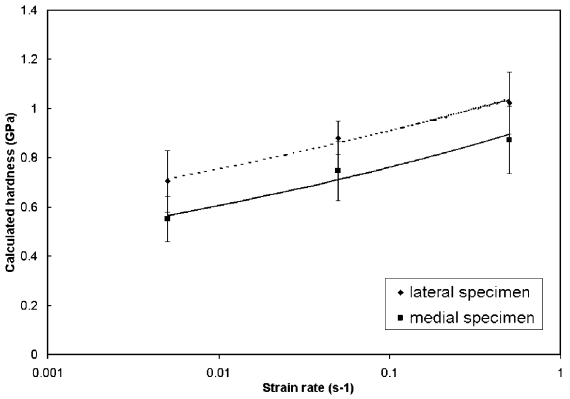

FIG. 5. Variation of calculated hardness as a function of strain rate in bone specimens (average values from 2000 to 3000 nm indentation depth; error bars correspond to the standard deviation).

However, the discrepancy of the comparison found for Young's modulus at the different strain rates is a singular phenomenon and should be confirmed by increasing the number of tests and specimens.

Influence of strain rate on elastic properties have been investigated by Fan et al.[26] by quasistatic nanoindentation tests in osteon lamellae. Young's modulus was found to be a function of the strain rate raised to the 0.058 power. One should note that Fan et al. values were close to those found by Carter and Hayes at the macroscopic scale.[31,32]

Viscoplasticity of bone had not yet been investigated at the microstructural scale, as all nanoindentation protocols on bone were intended to minimize this viscoplastic effect. The aim of our study was to evaluate this phenomenon. Our results exhibited a variation of the hardness as a function of the strain rate. Consequently, a viscoplastic behavior was stated at the micrometer scale in the interstitial bone. However, in the CSM technique used in the present study, the Young's modulus was calculated from the harmonic response of the material at a constant frequency of 45 Hz and for three different strain rates. According to the CSM method,[14,16] Young's modulus should not be sensitive on the quasistatic strain rate loading but to the harmonic displacement frequency. As a consequence, the observed variation of Young's modulus with strain rates would be related to an inaccuracy of the estimation of the contact area.

From the Oliver and Pharr model:

$$E = \frac{\sqrt{\pi}}{2} \times S \times A^{-1/2} \quad , \tag{5}$$

$$H = \frac{L}{A} \quad , \tag{6}$$

where E is Young's modulus, S is contact stiffness, H is hardness, A is contact area, and L is load.

From the present study:

$$E = k_1 \times \dot{\epsilon}^{n} \quad , \tag{7}$$

$$H = k_2 \times \dot{\epsilon}^{n'} \quad . \tag{8}$$

From Eqs. (5) and (7):

$$A - k_3 \times \dot{\epsilon}^{-2n} \quad . \tag{9}$$

The corrected value of the n power on Young's modulus calculation implied a correction of $2n$ on contact area formula. This implied a correction of the viscoplastic coefficient n' to $n' - 2n$. As a consequence, from Eqs. (6) and (8), the hardness relationship with strain rate became:

$$H = k_4 \times 2\dot{\epsilon}^{(n'-2n)} \quad , \tag{10}$$

where k_1, k_2, k_3, k_4 are constant values.

The viscoplastic coefficients were reduced to 0.029 and to 0.035 for the lateral and medial specimens, respectively. Our results suggested that the viscoplastic behavior should not be neglected in bone behavior investigations at the microscopic scale. In the present study, a ten-fold increase of the strain rate applied during the indentation had an impact of 6.9% and 8.4% on the hardness calculated for the lateral and medial specimens respectively. To our knowledge, it is the first time that this behavior is described at the microstructural level. This phenomenon may reflect the impact of the organic component in the mechanical behavior of the bone matrix. In fact, at the macroscopic scale, the time-dependent behavior has been observed to be mostly related to the collagen matrix behavior.[33] Moreover, chemical bonds between fibrils were suspected to be hydrogen bonds and strongly related to the water content of the bone matrix. In addition to the organic matrix, the apatite crystal organization and their interactions with the collagen matrix are poorly understood.[1]

V. CONCLUSION

The present study shows the relevance of the time-dependent behavior of bone at the microstructural scale. A viscoplastic behavior was described at the microscopic scale for the first time. This behavior may be related to the role of the organic component in the mechanical behavior of the bone matrix.

Understanding of the mechanical behavior of bone matrix remains to be developed at the microstructural scale. Further investigations of the interactions of organic and mineral parts and their consequences on the mechanical behavior on the bone matrix should be performed in that matter.

ACKNOWLEDGMENTS

This study was supported by the French "Ministère de l'Education Nationale, de l'Enseignement Supérieur et

de la Recherche" through the "Programme PluriFormation, Nanobiotechnologies" and by the French national scientific research center Centre National de la Recherche Scientifique (CNRS) and the French national institute of Health Institut National de la Santé Et de la Recherche Médicale (INSERM) through a joint program IT2B "Ingénierie Tissulaire Biomécanique et Biomatériaux."

REFERENCES

1. J.Y. Rho, L. Kuhn-Spearing, and P. Zioupos: Mechanical properties and the hierarchical structure of bone. *Med. Eng. Phys.* **20,** 92 (1998).
2. D.T. Reilly, A.H. Burstein, and V.H. Frankel: The elastic modulus for bone. *J. Biomech.* **7,** 271 (1974).
3. D.T. Reilly and A.H. Burstein: The elastic and ultimate properties of compact bone tissue. *J. Biomech.* **8,** 393 (1975).
4. J.D. Currey: The mechanical properties of bone. *Clin. Orth. Relat. Res.* **73,** 210 (1970).
5. J.D. Currey: The effect of porosity and mineral content on the Young's modulus of elasticity of compact bone. *J. Biomech.* **21,** 131 (1988).
6. P. Zioupos and J.D. Currey: Changes in the stiffness, and toughness of human cortical bone with age. *Bone* **22,** 57 (1998).
7. R.B. Ashman, S.C. Cowin, W.C. Van Buskirk, and J.C. Rice: A continuous wave technique for the measurement of the elastic properties of cortical bone. *J. Biomech.* **17,** 349 (1984).
8. S.S. Mehta, O.K. Öz, and P.P. Antich: Bone elasticity and ultrasound velocity are affected by subtle changes in the organic matrix. *J. Bone Miner. Res.* **13,** 114 (1998).
9. S. Bensamoun, J-M. Gherbezza, J-F. de Belleval, and M-C. Ho Ba Tho: Transmission scanning acoustic imaging of human cortical bone and relation with the microstructure. *Clin. Biomech. (Bristol, Avon).* **19,** 639 (2004).
10. A. Ascenzi and E. Bonucci: The tensile properties of single osteons. *Anat. Rec.* **158,** 375 (1967).
11. A. Ascenzi and E. Bonucci: The compressive properties of single osteons. *Anat. Rec.* **161,** 377 (1968).
12. A. Ascenzi, P. Baschieri, and A. Benvenuti: The bending properties of single osteons. *J. Biomech.* **23,** 763 (1990).
13. A. Ascenzi, P. Baschieri, and A. Benvenuti: The torsional properties of single selected osteons. *J. Biomech.* **27,** 875 (1994).
14. W.C. Oliver and G.M. Pharr: An improved technique for determining hardness and elastic modulus using load and displacement sensing indentation experiments. *J. Mater. Res.* **7,** 1564 (1992).
15. B.N. Lucas, W.C. Oliver, G.M. Pharr, and J-L. Loubet: Time dependent deformation during indentation testing, in *Thin Films: Stresses and Mechanical Properties VI,* edited by W.W. Gerberich, H. Gao, J-E. Sundgren, and S.P. Baker (Mater. Res. Soc. Symp. Proc. **436**, Pittsburgh, PA, 1997), p. 233.
16. A.C. Fisher-Cripps: *Nanoindentation,* 2nd ed. (Springer-Verlag, New York, 2004).
17. J.Y. Rho, T.Y. Tsui, and G.M. Pharr: Elastic properties of human cortical and trabecular lamellar bone measured by nanoindentation. *Biomaterials* **18,** 1325 (1997).
18. J.Y. Rho, P. Zioupos, J.D. Currey, and G.M. Pharr: Microstructural elasticity and regional heterogeneity in human femoral bone of various ages examined by nanoindentation. *J. Biomech.* **35,** 189 (2002).
19. P.K. Zysset, X.E. Guo, C.E. Hoffler, K.E. Moore, and S.A. Goldstein: Elastic modulus and hardness of cortical and trabecular bone lamellae measured by nanoindentation in the human femur. *J. Biomech.* **32,** 1005 (1999).
20. J.Y. Rho, P. Zioupos, J.D. Currey, and G.M. Pharr: Variation in the individual thick lamellar properties within osteons by nanoindentation. *Bone* **2,** 295 (1999).
21. C.E. Hoffler, K.E. Moore, K. Kozloff, P.K. Zysset, M.B. Brown, and S.A. Goldstein: Heterogeneity of bone lamellar-level elastic moduli. *Bone* **26,** 603 (2000).
22. S. Hengsberger, G. Boivin, and P.K. Zysset: Morphological and mechanical properties of bone structural units: A two case study. *JSME Int. J.* **45,** 936 (2002).
23. S. Hengsberger, A. Kulik, and P. Zysset: Nanoindentation discriminates the elastic properties of individual human bone lamellae under dry and physiological condition. *Bone* **30,** 178 (2002).
24. Z. Fan, J.G. Swadener, J.Y. Rho, M.E. Roy, and G.M. Pharr: Anisotropic properties of human tibial cortical bone as measured by nanoindentation. *J. Orth. Res.* **20,** 806 (2002).
25. S. Hengsberger, J. Enstroem, F. Peyrin, and P.K. Zysset: How is the indentation modulus of bone tissue related to its macroscopic elastic response? A validation study. *J. Biomech.* **36,** 1503 (2003).
26. Z. Fan and J.Y. Rho: Effects of viscoelasticity and time-dependent plasticity on nanoindentation measurements of human cortical bone. *J. Biomed. Mater. Res.* **67A,** 208 (2003).
27. K. Tai, H.J. Qui, and C. Ortiz: Effect of mineral content on the nanoindentation properties and nanoscale deformation mechanisms of bovine tibial cortical bone. *J. Mater. Sci.: Mater. Med.* **16,** 947 (2005).
28. J.Y. Rho and G.M. Pharr: Effects of drying on the mechanical properties of bovine femur measured by nanoindentation. *J. Mater. Sci.: Mater. Med.* **10,** 485 (1999).
29. C.E. Hoffler, X.E. Guo, P.K. Zysset, and S.A. Goldstein: An application of nanoindentation technique to measure bone tissue lamellae properties. *J. Biomech. Eng.* **127,** 1046 (2005).
30. G. Hochstetter, A. Jimenez, and J.L. Loubet: Strain-rate effects on hardness of glassy polymers in the nanoscale range—Comparison between quasi-static and continuous measurements. *J. Macromol. Sci., Phys.* **B38,** 681 (1999).
31. D.R. Carter and W.C. Hayes: Bone compressive strength: The influence of density and strain rate. *Science* **194,** 1174 (1976).
32. D.R. Carter and W.C. Hayes: The compressive behaviour of bone as two-phase porous structure. *J. Bone Joint Surg. Am.* **59,** 954 (1977).
33. N. Sasaki and M. Yoshikawa: Stress relaxation in native and EDTA-treated bone as a function of mineral content. *J. Biomech.* **26,** 77 (1993).